CORROSION SCIENCE AND TECHNOLOGY, Vol.7, No.2(2008), pp.85~91

Contribution of Water Chemistry in Initiation of Some Accelerated Corrosion Processes in CANDU-PHWR Primary System

Ioana Pirvan†, Maria Radulescu, and Manuela Fulger

Institute for Nuclear Research, Pitesti-P.O. Box 78, ROMANIA

By operation in aqueous environment at high temperature and pressure, the structural materials from Primary Heat Transport System (PHTS) cover with protective oxide films, which maintain the corrosion rate in admissible limits. A lot of potential factors exist, which conduct to degradation of the protective films and consequently to intensification of the corrosion processes. The existing experience of different nuclear reactors shows that the water chemistry has an important role in integrity maintaining of the protective oxide films. To investigate the influence of water chemistry (pH, O2 dissolved, Cl^-, F^-) on corrosion of some structural materials (carbon and martensitic steel, Zr and Ni alloys) and to establish the maximum permissible values, corrosion experiments by static autoclaving and electrochemical methods were performed. The experimental results allowed us to establish the contribution of the water chemistry in initiation and evolution of some accelerated corrosion processes.

Keywords *: accelerated corrosion, pitting corrosion, carbon steel, martensitic steel, Zr alloy, Ni alloy*

1. Introduction

The primary heat transport environment-heavy water in CANDU Reactor-is kept alkaline (at approximately pH= 10.2-10.4) by using LiOH in order to minimize the flow accelerated corrosion of carbon steel feeders, the deposition of the magnetite in core and the activity transport by minimizing crud formation. Also, to minimize the oxidation and hydriding of Zr alloys, the pitting corrosion of carbon and martensitic steel and cracking of stainless steel, the concentration of O_2 dissolved, Cl- and F- are maintained below the permissible limits.

During operation of nuclear reactor it is possible the environment contamination by several modalities:

- water radiolysis which can produce a increase of dissolved oxygen concentration in environment;
- degradation of the ions exchange resins, which can conduct to contamination with Cl^-;
- degradation of the fuel elements sheaths, which conducts to contamination which F^- ions originated by nuclear fission fuel (UO_2), which contains 340-560 ppm F^- as CaF_2;
- fluorine based components (flouro-carbon plastics) which are used in the primary system and which can degrade with high temperature resulting in appreciable fluoride in the primary coolant.

Also, presence of the crevices can involve certain conditions, when the pH-value can rise to 11.5 and 12-12.5 "From the report 1)".

To understand the contribution of water chemistry in initiation of some accelerated corrosion processes in CANDU-6 Reactor primary system, intensive corrosion experiments were executed.

2. Experimental

To investigate the water chemistry effects on characteristics of corrosive films formed on different structural materials, a lot of corrosion experiments by electrochemical methods and static autoclaves were performed.

The electrochemical determinations were performed by:

- potentiostatic method in LiOH solution (pH=10÷12), at room temperature;
- potentiodinamic and cyclic polarization method in LiOH solution (pH=10÷12), at room temperature and 80℃;
- cyclic polarization in LiOH (pH=10.5) with different concentrations of Cl^- and F^- (0.1; 0.5; 1; 10; 50 and 100 ppm), at room temperature, at 80℃ and 90℃.

The corrosion experiments at high temperature (310℃) and pressure (9.8 MPa) were performed in "Prolabo" and "Baskerville" static autoclaves, in the following solutions:

† Corresponding author: ipirvan@nuclear.ro

- LiOH degassed solution with (pH=10÷12.5);
- LiOH degassed solution (pH=10.5) and contaminated with Cl^- and F^- in concentration of 0.1÷100 ppm (0.1; 0.5; 1; 5; 10; 50 and 100 ppm), proceeding from NaCl and NaF;
- LiOH degassed solution (pH=10.5) with oxygen dissolved in concentration of 0.1÷500 ppm (0.1; 1; 10; 100 and 500 ppm), obtained by addition of H_2O_2

The coupons were cut from Zircaloy-4 sheaths, Zr-2.5%Nb tubes, carbon steel SA 106 gr. B and martensitic steel 403 m tubes and Incoloy-800 tubes. The initial surface of the coupons was no oxidized (degreased in organic solvents) and preoxidized with an oxide of thickness about 0.8 μm and 1.5 μm, formed at high temperature and pressure.

The post-testing analysis of the corrosive films was performed by gravimetric analysis, optical and electron microscopy examinations, as well as XRD, XPS and electrochemical impedance spectroscopy (EIS) determinations.

3. Results and discussion

3.1 Effect of LiOH solution pH

The excessive lithium hydroxide concentrations raising the pH above 11.5 accelerated the pre-transition corrosion rate and oxidation of Zirconium alloys. Thus, for Zr-2.5%Nb coupons tested at 310℃ (9.8 MPa) in LiOH solution with pH=12.5, the slope of the kinetic curve raised significantly after only 20 testing days and the corrosion process developed in post-transition period (Fig. 1a).

Oxidation along the grain boundaries in a pressurized lithiated water solution at pH<11.5 was not as pronounced as in a pressurized lithiated solution with pH=12-12.5.

The protective oxide layer, formed in LiOH solution at pH=10.5, consisted mainly of amorphous and tetragonal ZrO_2. The re-crystallization process in the oxide layer was altered by presence of LiOH causing a smaller grain size in oxide and a more rapid transition from the tetragonal oxide phase to the monoclinic phase.

The oxides, obtained after 30 testing days in LiOH solution with pH=12.5, were gray-light with no-uniform and porous aspect and their thickness increased from 1-2 μm (pH=10.5-100 testing days) to 18-25 μm (Fig. 1b).

Morphologically, these oxides differed from the black and uniform oxides, obtained in LiOH with pH=10.5, having a layered oxide structure with different pore sizes (Fig. 2) "From the report 2)".

XPS examination of a thick, no-uniform, white and pulverulent oxides emphasized the presence of Li^+, LiOH and lithium zirconate in oxide lattice (Fig. 3). The incorporation of Li^+ in zirconium oxide lattice conducted to a bigger concentration of anionic defects produced by Zr^{4+} ions substitution with Li^+ ions in oxide, increasing oxygen diffusion through oxide.

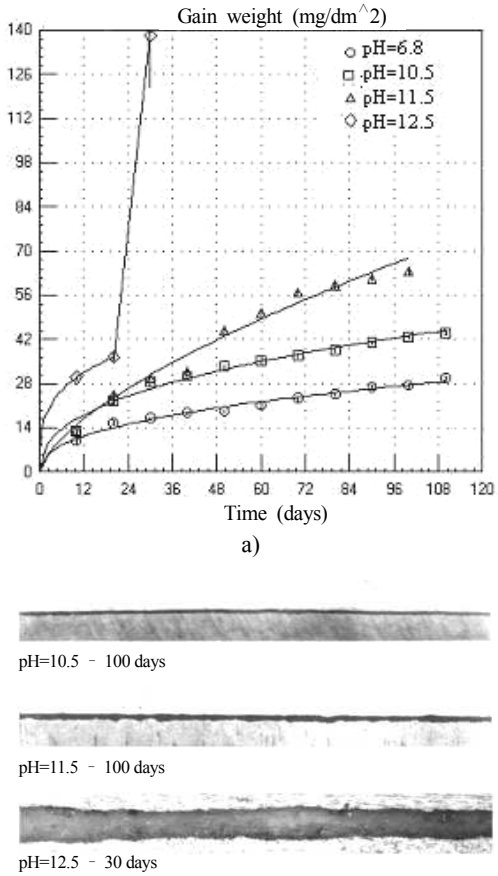

Fig. 1. Corrosion kinetic and oxides aspect of Zr-2.5%Nb alloy tested in LiOH solutions at 310℃ (9.8 MPa)

Fig. 2. Morphology of oxide film formed on Zr-2.5%Nb tested 30 days in LiOH- pH=12.5 (x1000)

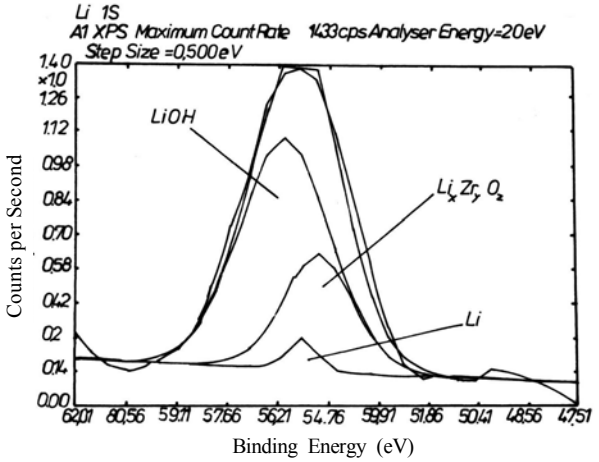

Fig. 3. XPS spectrum on Zr-2.5%Nb tested 30 days in LiOH-pH=12.5

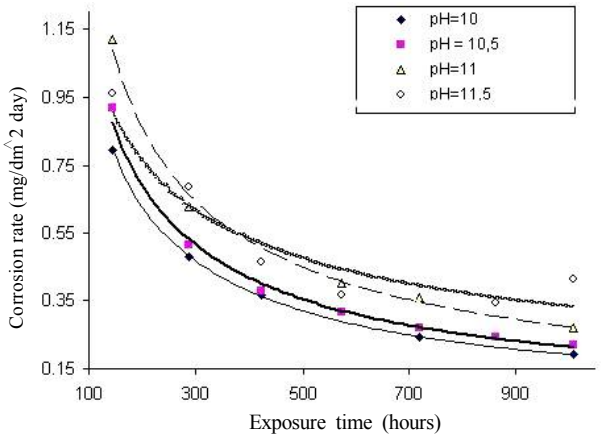

Fig. 4. Corrosion kinetics of carbon steel coupons tested at 310℃ (9.8 MPa) in LiOH

The corrosion rate of carbon steel SA 106 gr. B and martensitic steel 403m coupons, tested at high temperature and pressure, increased with LiOH solution pH (Fig. 4).

At pH=11.5 the oxide films were no uniform, porous and no adherent. Their thickness increased with pH of LiOH solutions, from 1-1.5 μm for pH=10.5 to about 6÷8 μm for carbon steel SA 106 gr. B and 3-4 μm for martensitic steel 403 m, after 30 testing days at 310℃.

The electrochemical impedance spectroscopy determinations showed that the oxide films formed on coupons tested in LiOH solution with pH=11 and 11.5 had a low capacitive behavior and were less protective than those formed in LiOH solution with pH=10.5, because the penetration of electrolyte in the oxide layer conducted to important modifications in the shape of Bode curves, after different periods from immersion moment in solution (Fig. 5).

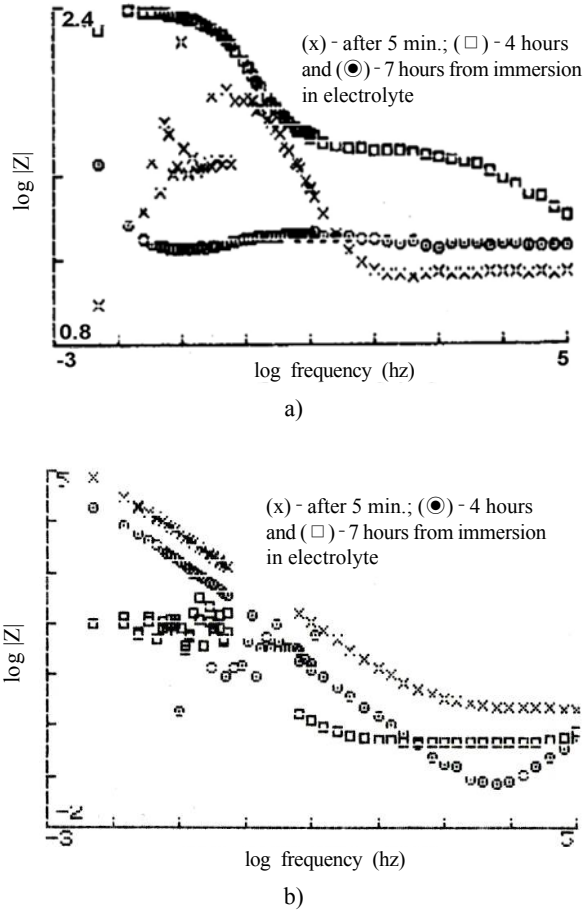

Fig. 5. Bode curves corresponding to the oxide films formed at 310℃ (9.8 MPa on carbon steel SA 106 gr.B in LiOH-pH=11.5 (a) and martensitic steel 403 m in LiOH-pH=11 (b) coupons after 60 testing days)

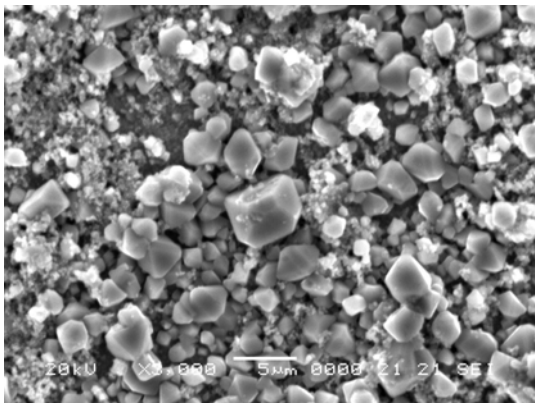

Fig. 6. Morphological analysis of the porous film (x3000)

The morphological analysis of the porous oxide films showed that they contain beside big octahedral magnetite crystals and smaller hematite crystals (Fig. 6).

By X-ray diffraction analysis, Fe and Li complex oxides

and more Fe_2O_3 were emphasized, on oxide films formed in LiOH solution with pH=11.5 "From the report 3)".

In the case of martensitic steel 403 m and Incoloy-800 alloy, the increase of LiOH solution at 11.5 and 12 conducted to acceleration of the generalized attack and appearance of some localized attack, in the shape of the superficial pits, due to changes in composition and structure of the oxide film. These pits, evidenced by formation of the hysterezis loop on cyclic polarization curves, are passived relatively quick and corrosion process is generalized.

EIS determinations showed that in LiOH solution with pH=12 were evidenced the formation on Iy-800 alloy of some corrosive films from two layers: the exterior oxide layer was porous and it had a low capacitive behavior and the internal oxide layer, from alloy interface, was compact and adherent.

The porous and non-adherent character of exterior oxide layer was due to prevalent formation of hematite film and compounds with Fe and Li, determined by XRD analysis.

The protective oxide films contained big magnetite crystals in octahedral or rhomboidal shape and smaller crystals of $NiFeO_4$ or $Ni_xFe_{3-x}O_4$ spinels (Fig. 7). The internal oxide layer, from metallic interface, is enriched in chromium and acts as a diffusion barrier.

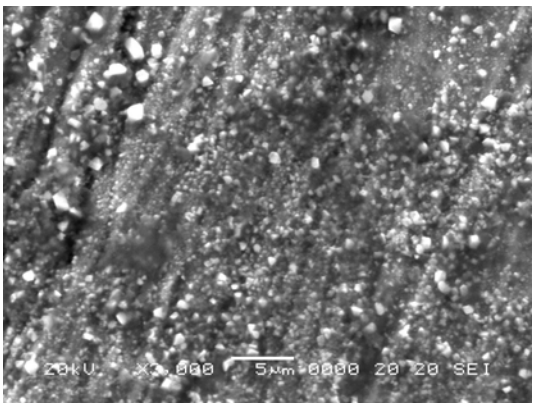

Fig. 7. Morphological analysis of the protective corrosive film on Incoloy-800 coupons (x 3000)

The chemical charts evidenced that Cr distribution follows the form of Fe distribution, this suggesting the existence of the chemical bound between Fe and Cr. This observation is in concordance with existence of spinel type oxide ($FeCr_2O_4$) evidenced by XPS analysis.

The imperfect duplex oxide films formed in abnormal water chemistry conditions (LiOH solution with pH=12) corresponded to a "passive pit" model with local damages in the exterior layer (Fig. 8). Warburg impedance (Z_w) and the constant phase element ($Q_{ext.}$) show that in the porous exterior layer, the diffusion process of the ionic specieses from solution by the imperfections of the film is prevalent.

3.2 Effect of halogens (Cl^-, F^-)

The contamination of the primary coolant with more than 0.2 ppm Cl^- and 0.1 ppm F^- accelerated the oxidation and hydriding of Zr alloys, as well as corrosion of carbon and martensitic steel and Incoloy-800 alloy.

The corrosion process in presence of Cl^- and F^- was initiated by pitting corrosion, the phenomenon being more emphasized in presence of Cl^- (Fig. 9).

In presence of F^- high concentration, Zy-4 alloy was more susceptible than the Zr-2.5%Nb at an accelerated oxidation undergoing simultaneously a more severe hydriding.

The pitting corrosion on carbon steel SA 106 gr. B appeared after 12 testing days in solution with 0.5 ppm Cl^-

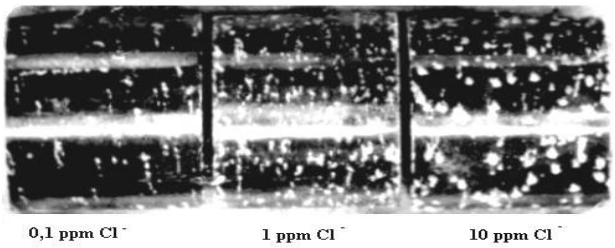

Fig. 9. Aspect of Zircaloy 4 coupons tested 72 hours by autoclaving at 400℃ (10 MPa) after electrochemical testing at 20℃ in presence of Cl^- (x2)

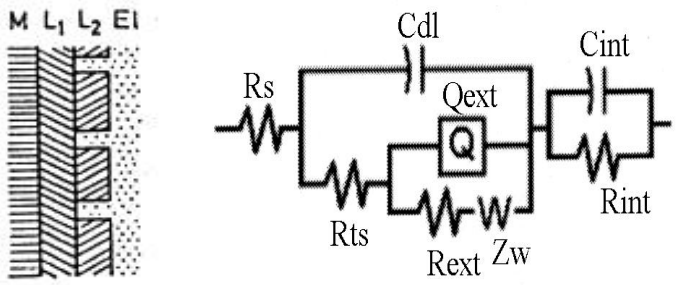

Rs (solution resistance) = 1E2Ωcm^2
Cdl (electrochemical double layer capacitance) =1.812E-10 F/cm^2
Rts (charge transfer resistance) =1098Ωcm^2
Qext (constant phase element) =2.1E-4S sec$^{0.79}$/cm^2
Rext (exterior layer resistance) =1221Ωcm^2
W (Warburg impedance) = 6.06E-5Ssec$^{0.5}$/cm^2
Cint (internal layer capacitance)= 1.087E-5F/cm^2
Rint (internal layer resistance)= 74.2Ωcm^2

Fig. 8. Equivalent electrical circuit for imperfect duplex oxide film

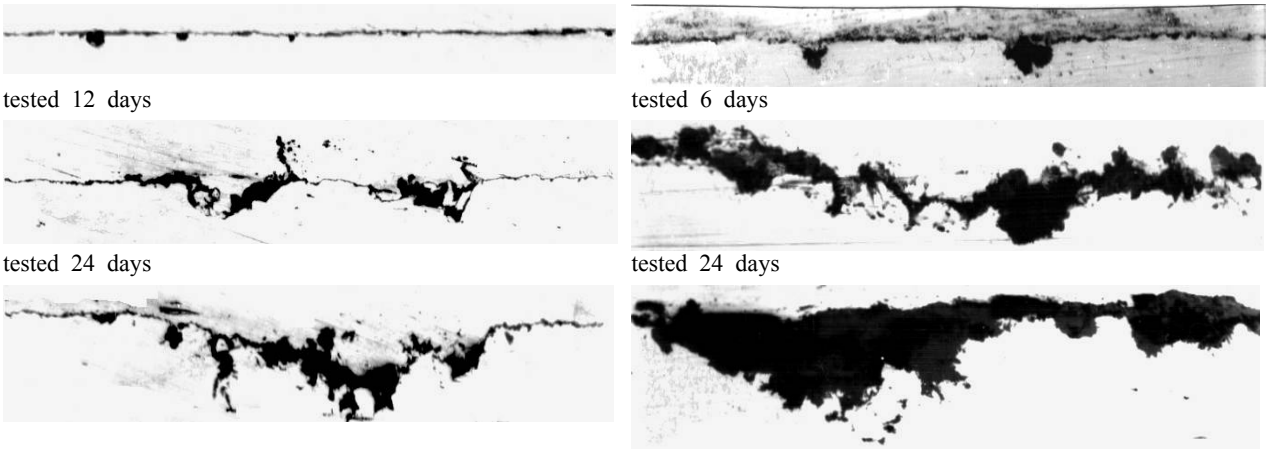

a) LiOH solution (pH=10.5) with 0.5 ppm Cl^- b) LiOH solution (pH=10.5) with 1 ppm Cl

Fig. 10. Pitting corrosion on carbon steel SA 106 gr. B coupons tested at 310℃ (9.8 MPa) (x 250)

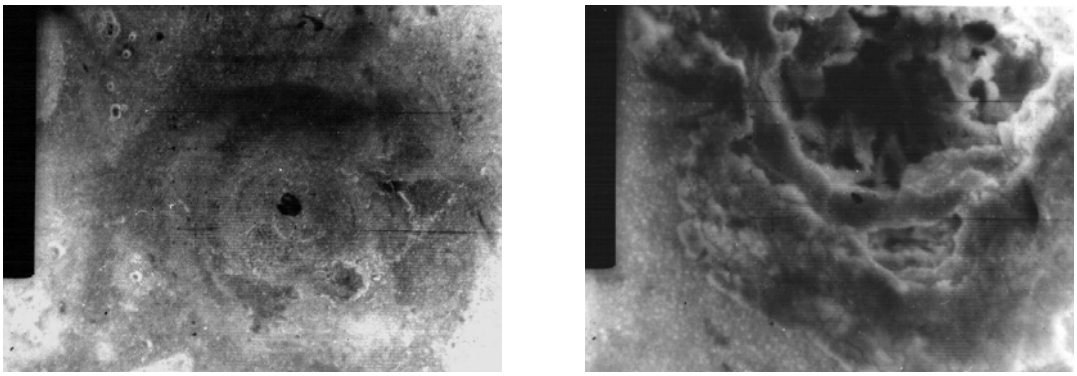

a) (x60) b) (x800)

Fig. 11. Morphological analysis of the pits formed on carbon steel tested 24 days, in LiOH with 1ppm Cl^-

and after 6 testing days in solution with 1 ppm Cl (Fig. 10a and b).

The corrosion process was characterized by the formation of some inhomogeneous corrosion product layers at the corroding surface, presenting active pits. The analysis of the structure in the zones with pits showed that: the localized attack isolated the zone of pit under film thickened; the surface from interior of the pit was no-uniform attacked, due to action of the chemical environment from pit, where the corrosion products could not protect metallic interface; the stronger pitting attack was in the zone having a structure with the bigger concentration in perlite.

By electron microscopy analysis a typical morphology of a localized attack by pitting corrosion was evidenced (Fig. 11a), but the morphology from interior of the pits (Fig. 11b) was determined by the strong attack of the metallic lattice, in the severe conditions from interior of the pits, which did not allow the passivation.

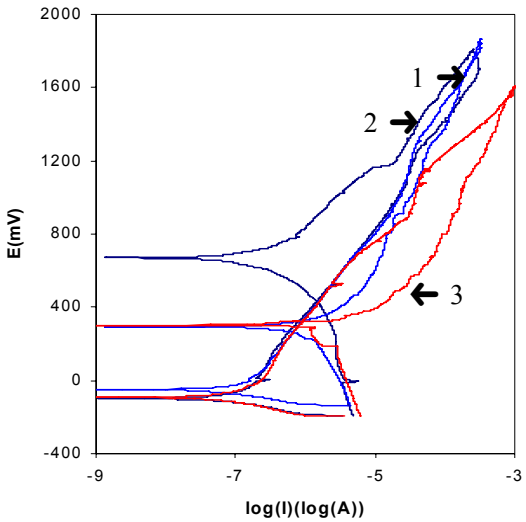

Fig. 12. Cyclic polarization curves on Iy-800 alloy at 25℃ in NaCl: (1)-0,5 ppmCl^-; (2)-1 ppmCl^- and (3)-10 ppmCl

The pitting corrosion on no-oxidized martensitic steel 403 m coupons appeared beginning with the concentration of 10 ppm Cl^-, but on no-oxidized Iy-800 alloy, the pitting corrosion was initiated beginning with the concentration of 1 ppm Cl^- at room temperature, (Fig.12).

Presence of an oxide layer, about 1.5 μm thickness, formed by static autoclaving time of 30 days in LiOH solution (pH=10.5) at 310℃ (9.8 MPa), delayed the apparition of the pitting corrosion on carbon, martensitic steel and Iy-800.

3.3 Effect of oxygen

The dissolved oxygen concentration of the water has a major importance in structural materials corrosion from primary circuit.

At oxygen concentration above 70 ppb (100 ppb) in presence of a neutron flux, an accelerated corrosion of Zircaloy-4 cladding has been observed, and is characterized by the formation of nodular type oxides "From the report 4)".White ZrO_2 nodules, with a diameter up to 4 mm and thickness up to 300 μm, having lenticular form were formed after 90 testing days at 310℃ (10.6 MPa) in INR TRIGA Reactor (Fig. 13 and 14).

An acceleration of Zr-2.5%Nb alloy corrosion at oxygen concentration above 0.1 ppm O_2 was observed (Fig. 15).

Fig. 13. Nodular corrosion on CANDU fuel element tested 90 days in INR TRIGA Reactor (x 1.5)

Fig. 14. Zirconium oxide nodule in section (x 40)

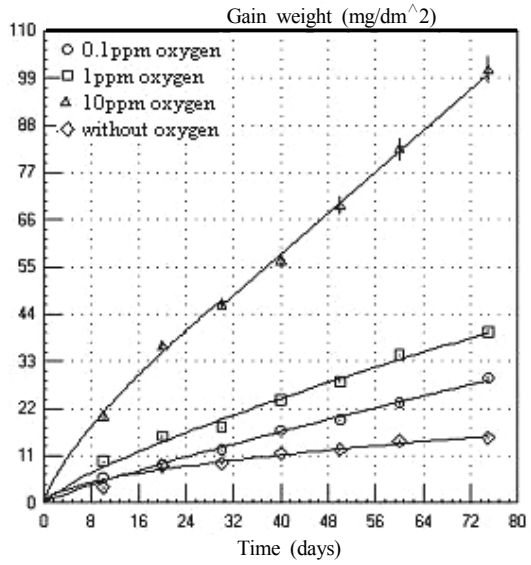

Fig. 15. Corrosion kinetics of Zr-2.5%Nb coupons tested at 310℃ in LiOH solution (pH=10.5) with oxygen

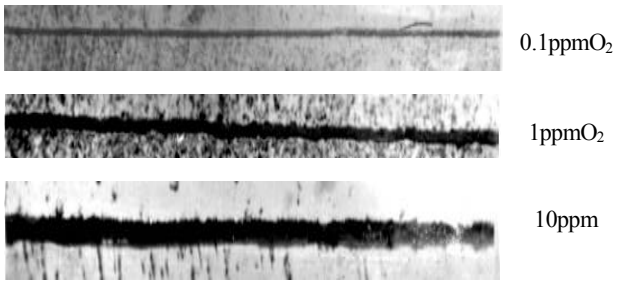

Fig. 16. Aspect of oxides formed on Zr-2.5%Nb coupons, tested 75 days at 310℃ in LiOH (pH=10.5) with oxygen (x500)

The accelerated oxidation of Zr-2.5%Nb alloy, at concentration of 10 ppm O_2, determined formation of thicker, no-homogenous and porous oxides (Fig. 16); the oxidation process being controlled by transport oxygen through diffusion.

In same testing conditions the evolution of Zr-2.5%Nb alloy hydriding was similarly with its oxidation conducting to increase of H_2 absorbed quantity in Zr-Nb matrix, and formation of some bigger hydrides.

Experiments performed in LiOH solution (pH=10.5) contaminated with oxygen evidenced that both at 100 ppm O_2 and 500 ppm O_2 appeared pitting corrosion on carbon steel SA 106 gr. B coupons. The corrosion rate in presence of 100 ppm O_2 was greater, due to a more intensive pitting corrosion (Fig. 17).

X-rays diffraction analysis evidenced that the films formed in environment with O_2 dissolved contained a bigger quantity of hematite (Fe_2O_3) and a smaller quantity

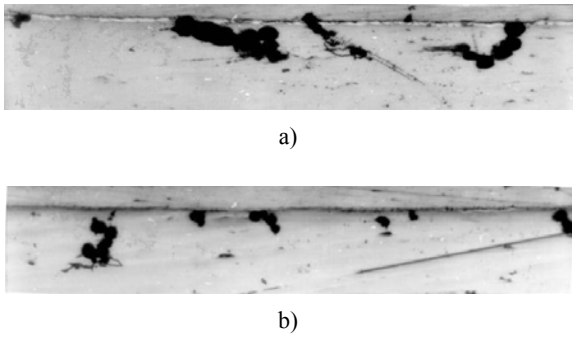

a)

b)

Fig. 17. Pitting corrosion on carbon steel SA 106 gr. B coupons after 60 testing days at 310℃ (9.8 MPa) in LiOH (pH=10.5) with: a) 100 ppm O_2 and b) 500 ppm O_2 (x 500)

of magnetite (Fe_3O_4). The magnetite was transformed into hematite, which being easily detachable, allowed the exposure of metallic under layer at very high subsequent corrosion "From the report 5)".

4. Conclusions

1) Excessive lithium hydroxide concentrations raising the pH above 11 accelerates the corrosion of structural materials, because of the possible formation of lithium zirconate, and conducts to formation of some porous and no adherent oxide films, as well as to appearance of the local attacks on martensitic steel and Incoloy-800.

2) The growth of O_2 concentration beyond the specified value accelerates oxidation and hydriding of Zr-2.5%Nb and points to the danger of uniform corrosion because of oxidizing effect of ferric deposits, as well as for the appearance of the pitting corrosion in the primary circuit structural materials.

3) Chloride and fluoride concentrations are important control parameters in water chemistry, because of the influence on stress corrosion cracking in stainless steels and Incoloy-800 and pitting corrosion in carbon and martensitic steel, Zr. and Iy-800 alloys.

4) The pitting corrosion determined the formation of some non-protective oxide films and inhomogeneous surfaces, as well as a local removal of material in shape of pits

References

1. D. H. Lister, "*Corrosion in Primary Coolant Systems*", IAEA-TEC-DOC-667, **2**, (1992).
2. I. Pîrvan, M. Rădulescu, L. Velciu, *Proceedings of the 5th Inter.Sem. on Primary and Secondary Side of Nuclear Power Plants*, Hungary, (2001).
3. I. Pîrvan, M. Rădulescu, A. Dinu, *Chemistry Rev*., **53**, 8 (2002).
4. M. Pîrvan, L. Stamatescu, T. Crăciunescu, "Nondestructive Post-Irradiation Examination of A08 Fuel Element Irradiated in INR TRIGA Reactor" *INR Internal Report* no.2253.
5. I. Pîrvan, M. Rădulescu, "Influence of Oxygen on Carbon Steel Pipes Corrosion", *2nd Inter. Conference ISBN 973-672-799-9*, Romania (2003).